Health Scope. ; In Press(In Press): e144472. https://doi.org/10.5812/healthscope-144472.

Published online: 2024 April 24. **Research Article**

Removal of Pyrocatechol from Aqueous Solution Using Activated Carbon Coated with Aluminum Nanoparticles by a Green Method

Bahram Kamarehie [1], Ali Jafari [2,1], Faramarz Azimi [1], Marzieh Rashidipour [3], Arefeh Sepahvand [4,*]

[1] Environmental Health Research Center, Lorestan University of Medical Sciences, Khorramabad, Iran
[2] Department of Environmental Health Engineering, School of Public Health, Kermanshah University of Medical Sciences, Kermanshah, iran
[3] Razi Herbal Medicines Research Center, Lorestan University of Medical Sciences, Khorramabad, Iran
[4] Student Research Committee, Lorestan University of Medical Sciences, Khorramabad, Iran

[*] *Corresponding author:* Student Research Committee, Lorestan University of Medical Sciences, Khorramabad, Iran. Email: arefehsepahvand21@gmail.com

Received 2024 January 13; **Revised** 2024 February 20; **Accepted** 2024 February 24.

Abstract

Background: Pyrocatechol, a phenol derivative, is commonly found in industrial effluents at various concentrations due to its extensive use in multiple industries. These toxic compounds are resistant to biological degradation and pose significant threats to environmental and human health when they enter aquatic environments.

Objectives: This study explores the removal of pyrocatechol from aqueous solutions using activated carbon coated with aluminum nanoparticles.

Methods: Laboratory materials included oak wood (collected from the mountains around Lorestan province, Iran), pyrocatechol, H_3PO_4, HCl, Al_2O_3, NaCl, NaOH, graphite oxide, and NH_3. This experimental study was conducted on a laboratory scale. Oak wood was used to synthesize activated carbon, while aluminum oxide and oak moss were employed to produce aluminum nanoparticles using a green method. The characteristics of the adsorbents were examined using XRD, FESEM, FTIR, and BET analyses. Parameters such as contact time (5 - 40 min), pH (3 - 11), initial concentration of pyrocatechol (20 - 200 mg/L), adsorbent dose (50 - 250 mg), and ionic strength were investigated. The residual concentration of pyrocatechol was measured using a spectrophotometer at a wavelength of 275 nm.

Results: The results indicated that maximum adsorption efficiency was achieved with a pyrocatechol concentration of 100 mg/L, a pH of 7, a contact time of 20 minutes, and an adsorbent dose of 250 mg. Isotherm and kinetic analyses showed that the adsorption data correlated well with the Langmuir model and the pseudo-second-order kinetic model, respectively.

Conclusions: Activated carbon derived from oak wood and coated with aluminum nanoparticles using a green method is highly efficient in removing pyrocatechol from aqueous solutions. This method is recommended as an effective, rapid, cost-effective, and environmentally friendly approach for the removal of pyrocatechol from aqueous environments.

Keywords: Pyrocatechol, Activated Carbon, Adsorption Process, Oak Wood, Aluminum Nanoarticle, Green Method

1. Background

Pyrocatechol, a phenol derivative with the chemical formula 1,2-dihydroxybenzene ($C_6H_4(OH)_2$), is known for its synthesis through the hydroxylation of phenol using hydrogen peroxide. It is widely used in various industries including cosmetics, toiletries, dyeing, plastics production, photography, and pesticide synthesis. As a result, pyrocatechol is released into wastewater in varying concentrations from diverse industries such as chemical manufacturing and petroleum refineries, posing significant risks to human health and the environment due to its resistance to degradation, high persistence, and pronounced toxicity (1). Pyrocatechol can lead to kidney tubule damage, reduced liver function, neurological disorders, and the development of cancerous tumors. It is highly irritating to the eyes, skin, and respiratory system, and can cause DNA damage, liver dysfunction, coma, and even death (2). Its metabolites may also initiate several types of cancers. Recognizing the hazards associated with phenolic compounds, the United States Environmental

Protection Agency (EPA) has included phenols in its list of 126 priority toxic chemicals, leading to stringent regulations on phenol levels in water and wastewater by local authorities (3). The presence of pyrocatechol in drinking water sources and agricultural runoff poses a serious threat to the health of humans, animals, plants, and microorganisms. Therefore, it is crucial to purify wastewater containing pyrocatechol to protect public health and the environment (4). Various treatment methods have been used to remove phenolic compounds from water and wastewater, including advanced oxidation, solvent extraction, ion exchange, membrane processes, reverse osmosis, electrochemical methods, biological treatments, and adsorption. Among these, adsorption is recognized as a particularly effective and efficient method for removing both organic and inorganic pollutants from water and wastewater (5).

Adsorption stands out as a preferred choice due to its simple design, high efficiency, the possibility of adsorbent reuse, the absence of harmful by-products, accessibility, and comparability with other acceptable and implementable methods. Various adsorbents have been used in adsorption processes, including activated carbon, natural fibers, hematite, aluminum hydroxide, carbon nanotubes, zeolites, polymeric materials, and magnetic composites (6). Activated carbon, particularly that derived from agricultural residues such as walnut, pistachio, almond, pine, and oak, has shown effective removal of organic compounds from water and wastewater due to its accessibility, porosity, and high surface area (7). However, conventional adsorbents often exhibit low adsorption capacity. Consequently, in recent years, extensive research has been conducted to develop high-capacity and environmentally friendly adsorbents (8, 9). One approach to enhancing the adsorption capacity and reducing the environmental impact of natural adsorbents is the use of nanoparticles synthesized through green methods. Green synthesis utilizes extracts from various plants and their products for nanoparticle synthesis (10). Recently, plant extracts including those from black and green tea, grape and eucalyptus residues, and oak galls have been used to synthesize nanoparticles (11). Oak galls, rich in tannins, have seen increasing use since the 1950s as bacteriostatic agents, antitumor drugs, antioxidants, preservatives, water purification agents, and adsorbents, driven by ongoing research into the chemical structures and properties of plant tannins (8).

While various studies have explored adsorption processes with activated carbon, a review of scientific literature reveals no studies on the removal of pyrocatechol from water using activated carbon coated with aluminum nanoparticles synthesized by a green method.

2. Objectives

This research aimed to assess the removal efficiency of pyrocatechol from an aqueous solution using activated carbon coated with aluminum nanoparticles synthesized through a green method.

3. Methods

3.1. Materials

Oak wood and oak veneer were sourced from the mountains surrounding Lorestan province, Iran. Pyrocatechol (99% purity) was purchased from Sigma Aldrich (USA). Other chemicals used, including H_3PO_4 85%, HCl 37%, Al_2O_3 (99% purity), NaOH (99% purity), graphite oxide (99% purity), Tris(hydroxymethyl)aminomethane (99% purity), NaCl (99% purity), and NH_3 30%, were obtained from Merck (Germany). A 1000 mg/L standard solution of pyrocatechol was prepared by double distillation with distilled water and stored at 4°C. Desired concentrations were achieved through daily dilution of this standard solution (12).

3.2. Preparation of Powdered Activated Carbon

Oak wood was initially cut into pieces of 2 - 3 cm. The production of powdered activated carbon (PAC) involved three stages: Impregnation, carbonization, and activation. During the impregnation stage, the crushed materials were placed in an oven at 105°C for 24 hours. Carbonization occurred in an air-free environment by sealing and waxing the samples in an electric furnace at 600°C for 1 hour. The final activation stage was carried out using a chemical-thermal method. H_3PO_4 with a molarity of 1 was used for chemical activation, where the carbon produced was soaked in H_3PO_4 for 24 hours, followed by treatment in an oxygen-free environment at 700°C in a furnace for 2 hours. PAC was then milled and sieved to achieve particle sizes within 200 micrometers

(mesh size 70), washed several times with deionized water, and dried at 105°C for 2 hours (Figure 1) (13).

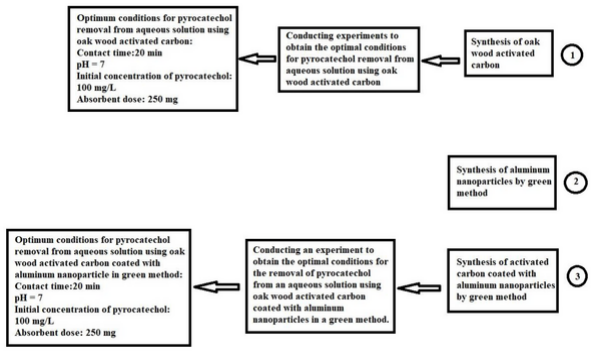

Figure 1. Schematic of the synthesis method of activated carbon adsorbent and activated carbon coated with aluminum nanoparticles using the green method.

3.3. Preparation of PAC Coated with Aluminum Nanoparticles (PAC-Al_2O_3)

Initially, 50 mL of a 1 mg/mL solution of graphene oxide was homogenized by ultrasonication for 5 minutes at 30°C. Subsequently, 20 mL of a solution containing 410 mg of aluminum oxide salt was added dropwise to the graphene oxide solution. This mixture was then heated in a water bath at 50°C for 15 minutes, and the pH was adjusted to 10 by adding 30% ammonia. The sample was placed back in a water bath at 85°C for 1 hour to complete the reaction. After the reaction, the solution was centrifuged at 10 000 rpm for 10 minutes, washed three times with deionized water and ethanol, transferred to a plate, and dried at 40°C for 24 hours. The aluminum oxide nanoparticles were then obtained by ultrasonication in 20 mL of deionized water for 10 minutes at 20°C. Subsequently, 0.2 mL of a 10 mg/mL aluminum oxide solution and 0.8 mL of a 10 mg/mL oak gall extract solution were added to the solution. The pH was adjusted to 8.5 with Tris buffer, mixed vigorously for 1 minute using a magnetic stirrer, transferred to a plate, and dried in an oven at 40°C for 48 hours. The resulting aluminum oxide nanoparticles were collected using a sterile blade (14).

Then, 52.55 g of aluminum oxide nanoparticles synthesized by the green method were dissolved in 1 liter of distilled water, and 3 mL of 1N NaOH was added under constant stirring. The mixture was stirred for 5 minutes, after which 50 g of activated carbon was added and gently stirred for 1 hour. The suspension was allowed to settle for 1 hour, and the supernatant was drained. The nanoparticle-coated activated carbon was then dried in an oven at 100°C for 1 hour. Subsequently, the material was placed in an electric furnace and heated at 500°C for 2 hours (15).

3.4. Adsorption Experiments

Batch adsorption experiments for pyrocatechol were performed using PAC in a closed system. The impact of various factors on the adsorption process was investigated using the one-factor-at-a-time method, involving 50 mL of solution and a shaker set to 250 rpm. After the adsorption process, the suspensions were centrifuged at 5000 rpm for 5 minutes, and the concentration of pyrocatechol in the liquid phase was determined using UV-Vis spectrophotometry at a wavelength of 275 nm (16). All experiments were conducted in triplicate, and the average values were recorded. The adsorption capacity (mg/g) of PAC was calculated using equation 1:

$$q_e = (C_0 - C_e)V/M \quad (1)$$

Where, q_e (mg/g) is the adsorption capacity of PAC, C_0 and C_e (mg/L) are the initial and final concentrations of pyrocatechol in the solution, V(L) is the volume of the solution, and M(g) is the mass of PAC.

3.5. Sample Preparation for BET Analysis

Initially, the samples were dried at temperatures ranging from room temperature to 300°C. This was followed by degassing the surface of the samples to remove potential water vapor, carbon dioxide, and other molecules that might have occupied the cavities of the material. Subsequently, the samples were exposed to liquid nitrogen at a constant temperature of 77 K, and specific, predetermined amounts of nitrogen were passed over the samples. The BET analysis was conducted using a BElSORP Mini model from Microtrac Bel Corp.

3.6. Characterization of Adsorbents

The crystalline size and specific surface area of the adsorbents were determined using X-ray diffraction (XRD) with an X' Pert Pro device from Panalytical company and BET analysis with a BElSORP Mini model

from Microtrac Bel Corp. Functional groups were analyzed using an FTIR device, Spectrum Two model from PerkinElmer, and morphological characteristics were examined with an FESEM device, ZEISS Sigma VP model, from Germany. The concentration of pyrocatechol in the solution was determined using a UV-Vis spectrophotometer at the maximum absorption wavelength of 275 nm.

3.7. Adsorption Isotherms

Adsorption isotherms define the mass of adsorbate absorbed per unit mass of adsorbent. In this study, the concentration of the absorbed substance was calculated using Equation 1.

3.7.1. Langmuir Isotherm

The Langmuir isotherm equation is expressed as follows:

$$q_e = \frac{Q_m K_L C_e}{1 + K_L C_e} \quad (2)$$

Where Q_m is the monolayer adsorption capacity, K_L is the Langmuir constant (mg/L), and other parameters have previously been defined.

3.7.2. Freundlich Isotherm

The Freundlich isotherm equation is given by:

$$q_e = K_f C_e^{\frac{1}{n}} \quad (3)$$

Where, n is the Freundlich intensity, K_f is the Freundlich capacity, and other parameters are already defined.

3.7.3. Adsorption Kinetics

To understand the dynamics of adsorption reactions, it is important to examine the information obtained from adsorption kinetics. In this study, two common types of kinetics were investigated.

4. Results and Discussion

4.1. Adsorbent Characteristics

The XRD pattern measured for PAC and PAC- Al_2O_3 is depicted in Figure 2. The diffraction peaks for PAC and PAC- Al_2O_3 appeared at angles of 21.84 and 29.33, respectively. The sharp peaks indicate excellent crystallinity of the prepared adsorbents, with two distinct peaks revealing the deposition and stable anchoring of aluminum oxide on the activated carbon.

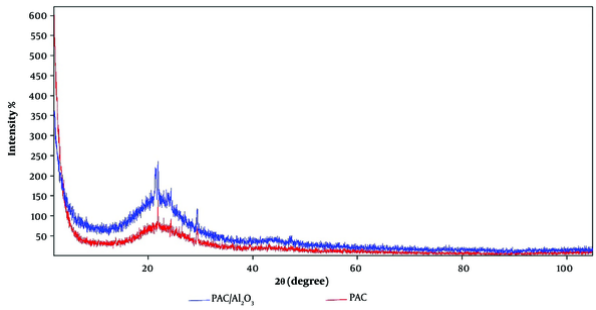

Figure 2. XRD image of PAC and PAC-Al_2O_3 adsorbent

Figure 3 displays FESEM images of the surface of activated carbon (A) and activated carbon coated with aluminum nanoparticles (B). The FESEM technique is utilized to analyze the surface size and morphology of the activated carbon and the nanoparticles stabilized on it. The images show a uniform coating of the activated carbon surface with spherical Al_2O_3 nanoparticles, which increases the contact surface and active sites on the activated carbon.

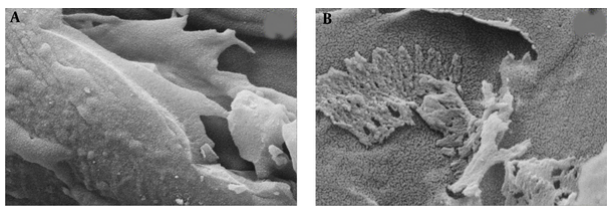

Figure 3. FESEM images of PAC (A) and PAC-Al_2O_3 adsorbent (B)

In Figure 4, FTIR images of Al_2O_3 nanoparticles and PAC-Al_2O_3 are shown. The absorbed peaks in the range of 3000 - 3400 cm^{-1} are attributed to the stretching O-H oscillation bands in the adsorbed water functional groups post chemical activation. The absorbed peaks within the 500 - 800 cm^{-1} range are associated with C-H

functional groups present in most organic compounds (17). Additionally, the absorption at the wavelength of 1112 cm^{-1} corresponds to the Al-O bonds of aluminum oxide nanoparticles immobilized on activated carbon. This result indicates that the deposition of Al_2O_3 on the activated carbon surface enhances the presence of Al-O functional groups and positively impacts the adsorbent's performance and the efficiency of the adsorption process (18).

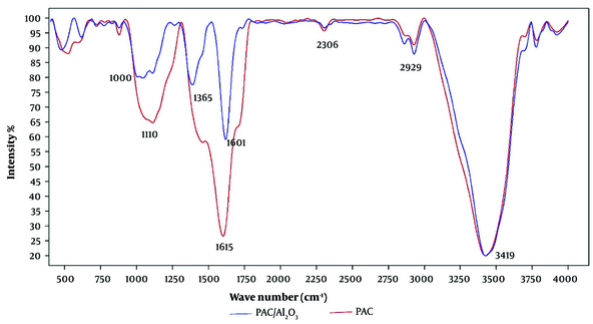

Figure 4. FTIR image of PAC and PAC-Al_2O_3 adsorbent

Table 1 presents the active surface area and pore size distribution using BET analysis for both PAC and Al_2O_3-stabilized nanoparticles on PAC (PAC-Al_2O_3). The results demonstrate that the nanoparticle coating on activated carbon increases the surface area and adsorbed volume, thereby improving the adsorbent's performance. The high surface area of the sample indicates that the resulting activated carbon is a suitable substrate for bonding with pollutants and facilitating their removal.

Table 1. BET Analysis Results for PAC and PAC-Al_2O_3 Adsorbent

Parameter	Unit	Concentration	
		PAC	PAC-Al_2O_3
BET	m^2/g	95.724	132.435
Total pore volume (P/P0 = 0.982)	cm^3/g	0.0936	0.1231
Monolayer volume, Vm	cm^3/g	24.759	28.819
Average pore diameter	nm	9.257	7.791

4.2. Impact of Contact Time on Adsorption

At the initial stage, the amount of pyrocatechol adsorbed on PAC and PAC-Al_2O_3 as a function of contact time (0 - 40 minutes) with a constant adsorbent amount of 100 mg and a solution pH of 7 at 20°C is shown in Appendix 1. The adsorption efficiency of pyrocatechol by PAC and PAC-Al_2O_3 increased to 73.58% and 95.64%, respectively, within the first 20 minutes. Subsequently, the removal rate and efficiency showed a diminishing trend, reaching equilibrium at about 75% and 95%, respectively. The initial increase in adsorption rate and efficiency can be attributed to the availability of active adsorption sites and increased surface contact between the functional adsorbent groups and pyrocatechol, leading to enhanced surface reactions (16). This observation is consistent with the findings of Rodrigues et al., who reported an increase in phenol removal efficiency with increasing contact time (19). Furthermore, a study by Tavengwa et al. demonstrated that adsorption with PAC was rapid in the early stages, achieving maximum value after 30 minutes (20).

4.3. Effect of Solution pH on Adsorption Efficiency

The solution pH significantly influences the properties of the adsorbent and adsorbate, affecting the adsorption process (21). It alters the surface characteristics of the adsorbent, the ionization degree of the adsorbate, and the type and state of ionic groups in both the adsorbent and adsorbate (22). The impact of solution pH (ranging from 3 to 11) on the adsorption of pyrocatechol using PAC and PAC-Al_2O_3 adsorbents is presented in Appendix 2. The data indicate that maximum adsorption of pyrocatechol by PAC (with a removal efficiency of 70.84%) and PAC-Al_2O_3 (with a removal efficiency of 89.81%) occurred at a pH of around 7. The point of zero charge (pH_zpc) for both AC and C-Al_2O_3 was approximately 7.4, and the degree of ionization of pyrocatechol with NaCl salt, calculated using Equation 4 with pKa values of 9.45 at pH values of 3, 7, 9, and 11, was 0.000035%, 0.35%, 26%, and 97%, respectively. These calculations indicated an increase in pyrocatechol ionization with increasing solution pH:

$$Capnization\% = \frac{100}{1 + 10^{pka - pH}} \quad (4)$$

The relative reduction in the adsorption capacity of adsorbents at pH values above 7.4 may be attributed to the adsorbent's negative surface charge and the electrostatic repulsion between the adsorbent and perchloroethylene ions. Conversely, at pH values below

7.4, the decrease in relative removal efficiency is due to the positively charged surface of the adsorbent, which leads to increased electrostatic adsorption and a reduction in ionization percentage (23). In a study conducted by Suresh et al. on the adsorption of catechol and resorcinol using granular activated carbon, it was noted that the efficiency of catechol removal increases with the pH rising from 2 to normal levels, then decreases drastically as the pH rises to 11.5 (24). Similarly, Yang and colleagues observed that the removal rate of nitrobenzene by ozone was very low at pH = 2, but increased with rising pH, aligning with the findings of the present study (25).

4.4. Effect of Initial Pyrocatechol Concentration

Appendix 3 illustrates the impact of varying initial pyrocatechol concentrations (20, 50, 100, 150, and 200 mg/L) on the removal efficiency using PAC and PAC-Al_2O_3 adsorbents. As depicted, the adsorption efficiency decreases with increasing initial concentration of pyrocatechol. The highest removal efficiency was observed at an initial concentration of 20 mg/L, achieving 98.04% with PAC and 99.98% with PAC-Al_2O_3. However, considering that a concentration of 100 mg/L is more typical in real wastewater, this concentration, with a removal efficiency of 70.84% using PAC and 89.81% using PAC-Al_2O_3, is chosen as the optimal concentration. As the initial concentration of pyrocatechol increases, the specific surface area and active functional groups per unit mass of the adsorbent decrease. Consequently, the removal efficiency diminishes due to the rapid saturation of adsorption sites, reduction of overlapping of adsorbent particles, and decreased effective surface area available for adsorption (26). This phenomenon aligns with the study conducted by Bazarafshan et al. on the removal of catechol using ZnO nanoparticles, where the removal efficiency decreased with an increase in the initial catechol concentration (27). Furthermore, the results of Arbabi et al.'s study showed that the adsorption of nitrate decreased as its initial concentration increased from 25 to 150 mg/L (28).

4.5. Influence of Adsorbent Dose on Adsorption

The results presented in Appendix 4 show a substantial increase in perchloroethylene removal efficiency for both PAC and PAC-Al_2O_3 adsorbents with an increase in adsorbent doses from 50 to 250 mg. Pyrocatechol adsorption increases with the increase of adsorbent dose due to the larger surface area of the adsorbent and the resulting increase in active surface adsorption sites (29). In this study, the adsorption efficiency of pyrocatechol for PAC and PAC-Al_2O_3 increased with the adsorbent dose, reaching maximum absorption efficiency at 250 mg/L of 94.65% for PAC and 99.97% for PAC-Al_2O_3. Therefore, this dose was determined as the optimum adsorbent dose. This phenomenon is further supported by the studies of Kumar et al., who investigated catechol removal using activated carbon derived from blue flag biomass. They reported that increasing the adsorbent dose from 0.5 to 1 g/L improved adsorption efficiency (30). Additionally, Suresh et al., in their study on the adsorption mechanism of catechol and resorcinol using granular activated carbon, reported an increase in removal efficiency from 22% to 74% at a concentration of 54.4 mmol/L and a contact time of 24 hours with a dose of 1 g/L (24). Furthermore, an increase in adsorbent quantity to more than 10 g/L led to a 98% removal efficiency, attributed to an increased surface area and more active groups on the adsorbent surface.

4.6. Adsorption Kinetics

Kinetic models are essential tools for determining the mechanism of pollutant removal using adsorbents (31). The examination of two kinetic models, first-order and second-order, revealed that the pyrocatechol adsorption process using PAC and PAC-Al_2O_3 adsorbents, with R^2 coefficients of 97% and 98% respectively, follows the pseudo-second-order kinetic model, as shown in Appendix 5. The pseudo-second-order kinetic is described by the Equation 5:

$$\frac{t}{q_t} = \frac{1}{k_2 q_e^2} + \frac{t}{q_e} \quad (5)$$

Where, q_e and q_t represent the adsorption capacity of the pollutant by the adsorbent at equilibrium and at time t (in g/g), respectively, and k_2 is the rate constant of the second-order kinetic model (g/mg.h). The values of k_2 and q_e are obtained from the slope and intercept of the plot of t/qt versus t, respectively (32). The adherence to a pseudo-second-order kinetic model indicates the involvement of various mechanisms, such as external film diffusion, intraparticle diffusion, and surface adsorption (33). It also signifies the suitability of the

pyrocatechol adsorption protocol in a porous medium. Mohd Din et al., in a study on phenol adsorption using activated coconut shell adsorbent, demonstrated that the adsorption kinetic model follows pseudo-second-order kinetics, with various factors significantly influencing the adsorption process (34).

4.7. Isotherm Study

Adsorption isotherms are crucial for understanding the interactions between the adsorbent and the adsorbate, playing an important role in optimizing the use of an adsorbent and determining its capacity. According to the results of adsorption reaction isotherm studies presented in Table 2, 3, and Appendix 6, both adsorption processes with activated carbon and activated carbon coated with nanoparticles displayed R^2 values for the Langmuir model of 0.9987 and 0.9958, respectively. Thus, the experimental data better align with the Langmuir isotherm. In the Freundlich model, the values of Kf and n indicate the adsorption strength, with the highest value of Kf corresponding to activated carbon coated with aluminum nanoparticles, and the highest value of n relating to activated carbon.

Table 2. Isotherm of Activated Carbon

Isotherm Type and Parameters	Values
Fraundlich	
n	2.5972
K_f	4.7845
R^2	0.5406
Langmuir	
K_L	0.7581
R^2	0.9987
q_m	26.6204

Table 3. Isotherm of Activated Carbon Coated with Aluminum Nanoparticles

Isotherm Type and Parameters	Values
Fraundlich	
n	1.5433
K_f	5.0054
R^2	0.5646
Langmuir	
K_L	0.1292
R^2	0.9958
q_m	84.6603

The KL values from the Langmuir models, which indicate the amount of ion adsorption needed to form a monolayer, were higher for activated carbon than for activated carbon coated with aluminum nanoparticles using the green method. This suggests that more amounts of the nanoparticle-coated activated carbon are required to form a monolayer, explaining why the adsorption capacity of the nanoparticle-coated activated carbon is higher than that of plain activated carbon. According to the Langmuir models in this study, the K_L values in the best absorption scenarios for activated carbon and nanoparticle-coated activated carbon were 0.7581 and 0.1292, respectively, indicating that pyrocatechol is adsorbed by the activated carbon adsorbent with more energy. The alignment with the Langmuir isotherm suggests that the adsorption occurs in a monolayer, indicative of a homogeneous distribution of active sites on the adsorbent's surface. The results of Kumar et al.'s study on the effective adsorption of catechol from aqueous solutions using activated carbon also followed the Langmuir isotherm (35).

4.8. Effect of Ionic Strength on Adsorption Efficiency

Ionic strength is crucial for the equilibrium of adsorbate and adsorbent in the liquid phase (36). Appendix 7 illustrates the impact of ionic strength (20, 40, 60, and 80 mg per L) on pyrocatechol removal efficiency using both adsorbents. The results show a decrease in adsorption efficiency with an increased concentration of solution ions. This phenomenon may be attributed to the electrostatic interactions between the adsorbent and adsorbate, which intensify with the increased ionic strength of the solution (37). Other researchers have also reported reduced pollutant removal efficiency due to increased ionic strength and electrostatic interactions between the adsorbent and adsorbate (38).

4.9. Conclusions

This study aimed to determine the removal efficiency of activated carbon derived from oak wood and coated with aluminum nanoparticles using a green method. The results demonstrated that oak wood activated carbon effectively removes pyrocatechol. This adsorbent, along with aluminum nanoparticles coated on it, enhances the removal of pyrocatechol. Adsorption by this adsorbent is higher at neutral pH. By increasing the contact time, reducing the initial concentration of

pyrocatechol, and increasing the adsorbent dose, the removal efficiency of pyrocatechol increases. The adsorption of pyrocatechol aligns with the Langmuir model, and pseudo-second-order kinetics is the best model for determining the reaction rate using activated carbon and activated carbon coated with aluminum nanoparticles. Given the high absorption capacity of pyrocatechol by activated carbon coated with aluminum nanoparticles synthesized via a green method, and considering that the adsorption capacity strongly depends on the pH of the solution, the initial concentration of pyrocatechol, adsorbent amount, and contact time, it is suggested that the optimal conditions of these variables be investigated for using this adsorbent in the removal of pyrocatechol on a larger scale and in real wastewater.

4.10. Limitations

- Conducting extensive trial and error to optimize the amount of activated carbon and nanoparticles in the synthesis of activated carbon coated with nanoparticles.

- Lack of sufficient financial resources to conduct tests with the HPLC device.

Acknowledgements

This article forms part of a Master's thesis in environmental health at Lorestan University of Medical Sciences. The present study is extracted from a dissertation with the ethics code IR.LUMS.REC.1400.293.

Supplementary Material

Supplementary material(s) is available here [To read supplementary materials, please refer to the journal website and open PDF/HTML].

Footnotes

Authors' Contribution: BK: Data collection, writing original draft preparation; AJ: Formal analysis; AS: Formal analysis; FA: Reviewing and Editing, MR: Reviewing and Editing.

Conflict of Interests: No conflicts of interest were declared by the authors.

Data Availability: No new data were created or analyzed in this study. Data sharing does not apply to this article.

Ethical Approval: The present study was taken from a dissertation with the code of ethics IR.LUMS.REC.1400.293 .

Funding/Support: This article was extracted from the thesis of Arefeh Sepahvand and has been financially supported by Lorestan University of Medical Sciences.

References

1. Abugazleh MK, Ali HM, Chester JA, Bouldin JL. Aquatic toxicity of hydroquinone and catechol following metal oxide treatment to ceriodaphnia dubia and pimephales promelas. *Ecotoxicol.* 2022. https://doi.org/10.21203/rs.3.rs-1497902/v1.
2. Bastos P, Gomes T, Ribeiro L. Catechol-O-Methyltransferase (COMT): An Update on Its Role in Cancer, Neurological and Cardiovascular Diseases. *Rev Physiol Biochem Pharmacol.* 2017;**173**:1-39. [PubMed ID: 28456872]. https://doi.org/10.1007/112_2017_2.
3. Cavalieri EL, Rogan EG, Chakravarti D. Initiation of cancer and other diseases by catechol ortho-quinones: a unifying mechanism. *Cell Mol Life Sci.* 2002;**59**(4):665-81. [PubMed ID: 12022473]. https://doi.org/10.1007/s00018-002-8456-0.
4. Samal K, Mahapatra S, Hibzur Ali M. Pharmaceutical wastewater as Emerging Contaminants (EC): Treatment technologies, impact on environment and human health. *Energy Nexus.* 2022;**6**. https://doi.org/10.1016/j.nexus.2022.100076.
5. Rathi BS, Kumar PS. Application of adsorption process for effective removal of emerging contaminants from water and wastewater. *Environ Pollut.* 2021;**280**:116995. [PubMed ID: 33789220]. https://doi.org/10.1016/j.envpol.2021.116995.
6. Samuel MS, Selvarajan E, Sarswat A, Muthukumar H, Jacob JM, Mukesh M, et al. Nanomaterials as adsorbents for As(III) and As(V) removal from water: A review. *J Hazard Mater.* 2022;**424**(Pt C):127572. [PubMed ID: 34810009]. https://doi.org/10.1016/j.jhazmat.2021.127572.
7. Lewoyehu M. Comprehensive review on synthesis and application of activated carbon from agricultural residues for the remediation of venomous pollutants in wastewater. *J Analytical Applied Pyrolysis.* 2021;**159**. https://doi.org/10.1016/j.jaap.2021.105279.
8. Bacelo HA, Santos SC, Botelho CM. Tannin-based biosorbents for environmental applications – A review. *Chemical Engineering Journal.* 2016;**303**:575-87. https://doi.org/10.1016/j.cej.2016.06.044.
9. Prajapati AK, Mondal MK. Comprehensive kinetic and mass transfer modeling for methylene blue dye adsorption onto CuO nanoparticles loaded on nanoporous activated carbon prepared from waste coconut shell. *J Molecular Liquids.* 2020;**307**. https://doi.org/10.1016/j.molliq.2020.112949.
10. Dikshit P, Kumar J, Das A, Sadhu S, Sharma S, Singh S, et al. Green Synthesis of Metallic Nanoparticles: Applications and Limitations. *Catalysts.* 2021;**11**(8). https://doi.org/10.3390/catal11080902.
11. Fazlzadeh M, Khosravi R, Zarei A. Green synthesis of zinc oxide nanoparticles using Peganum harmala seed extract, and loaded on Peganum harmala seed powdered activated carbon as new adsorbent for removal of Cr(VI) from aqueous solution. *Ecological Engineering.* 2017;**103**:180-90. https://doi.org/10.1016/j.ecoleng.2017.02.052.

12. Janes L, Lisjak K, Vanzo A. Determination of glutathione content in grape juice and wine by high-performance liquid chromatography with fluorescence detection. *Anal Chim Acta*. 2010;**674**(2):239-42. [PubMed ID: 20678636]. https://doi.org/10.1016/j.aca.2010.06.040.
13. Ao W, Fu J, Mao X, Kang Q, Ran C, Liu Y, et al. Microwave assisted preparation of activated carbon from biomass: A review. *Renewable and Sustainable Energy Reviews*. 2018;**92**:958-79. https://doi.org/10.1016/j.rser.2018.04.051.
14. Zhang G, Zhang R, Wang F. Fast formation kinetics of methane hydrates loaded by silver nanoparticle coated activated carbon (Ag-NP@AC). *Chemical Engineering Journal*. 2021;**417**. https://doi.org/10.1016/j.cej.2021.129206.
15. Moussavi G, Aghapour AA, Yaghmaeian K. The degradation and mineralization of catechol using ozonation catalyzed with MgO/GAC composite in a fluidized bed reactor. *Chemical Engineering Journal*. 2014;**249**:302-10. https://doi.org/10.1016/j.cej.2014.03.059.
16. Liu Q, Yang J, Li H, Ye J, Fei Z, Chen X, et al. Activated carbon prepared from catechol distillation residue for efficient adsorption of aromatic organic compounds from aqueous solution. *Chemosphere*. 2021;**269**:128750. [PubMed ID: 33199105]. https://doi.org/10.1016/j.chemosphere.2020.128750.
17. Hashemi F, Godini H, Khoramabadi GS, Mansouri L. [Assessing performance of walnut green hull adsorbent in removal of phenol from aqueous solutions]. *Iran J Health Environment*. 2014. Persian.
18. Velu M, Balasubramanian B, Velmurugan P, Kamyab H, Ravi AV, Chelliapan S, et al. Fabrication of nanocomposites mediated from aluminium nanoparticles/Moringa oleifera gum activated carbon for effective photocatalytic removal of nitrate and phosphate in aqueous solution. *J Cleaner Production*. 2021;**281**. https://doi.org/10.1016/j.jclepro.2020.124553.
19. Rodrigues LA, da Silva MLCP, Alvarez-Mendes MO, Coutinho ADR, Thim GP. Phenol removal from aqueous solution by activated carbon produced from avocado kernel seeds. *Chemical Engineering J*. 2011;**174**(1):49-57. https://doi.org/10.1016/j.cej.2011.08.027.
20. Jonglertjunya W, Lertchutimakul T. Equilibrium and kinetic studies on the adsorption of humic acid by activated sludge and Bacillus subtilis. *Songklanakarin J Sci Technol*. 2012;**34**(6).
21. Orfao JJ, Silva AI, Pereira JC, Barata SA, Fonseca IM, Faria PC, et al. Adsorption of a reactive dye on chemically modified activated carbons--influence of pH. *J Colloid Interface Sci*. 2006;**296**(2):480-9. [PubMed ID: 16298379]. https://doi.org/10.1016/j.jcis.2005.09.063.
22. Tamjidi S, Moghadas BK, Esmaeili H, Shakerian Khoo F, Gholami G, Ghasemi M. Improving the surface properties of adsorbents by surfactants and their role in the removal of toxic metals from wastewater: A review study. *Process Safety and Environmental Protection*. 2021;**148**:775-95. https://doi.org/10.1016/j.psep.2021.02.003.
23. Ahmed MB, Zhou JL, Ngo HH, Johir MAH, Sornalingam K. Sorptive removal of phenolic endocrine disruptors by functionalized biochar: Competitive interaction mechanism, removal efficacy and application in wastewater. *Chem Engineering J*. 2018;**335**:801-11. https://doi.org/10.1016/j.cej.2017.11.041.
24. Suresh S, Srivastava VC, Mishra IM. Study of Catechol and Resorcinol Adsorption Mechanism through Granular Activated Carbon Characterization, pH and Kinetic Study. *Separation Sci Technol*. 2011;**46**(11):1750-66. https://doi.org/10.1080/01496395.2011.570284.
25. Yang Y, Ma J, Qin Q, Zhai X. Degradation of nitrobenzene by nano-TiO2 catalyzed ozonation. *J Molecular Catalysis A: Chem*. 2007;**267**(1-2):41-8. https://doi.org/10.1016/j.molcata.2006.09.010.
26. De Gisi S, Lofrano G, Grassi M, Notarnicola M. Characteristics and adsorption capacities of low-cost sorbents for wastewater treatment: A review. *Sustainable Materials and Technologies*. 2016;**9**:10-40. https://doi.org/10.1016/j.susmat.2016.06.002.
27. Bazrafshan E, Al-Musawi TJ, Silva MF, Panahi AH, Havangi M, Mostafapur FK. Photocatalytic degradation of catechol using ZnO nanoparticles as catalyst: Optimizing the experimental parameters using the Box-Behnken statistical methodology and kinetic studies. *Microchemical J*. 2019;**147**:643-53. https://doi.org/10.1016/j.microc.2019.03.078.
28. Arbabi M, Hemati S, Shamsizadeh Z, Arbabi A. Nitrate removal from aqueous solution by almond shells activated with magnetic nanoparticles. *Desalination and Water Treatment*. 2017;**80**:344-51. https://doi.org/10.5004/dwt.2017.20999.
29. Toor M, Jin B, Dai S, Vimonses V. Activating natural bentonite as a cost-effective adsorbent for removal of Congo-red in wastewater. *J Industrial Engineering Chem*. 2015;**21**:653-61. https://doi.org/10.1016/j.jiec.2014.03.033.
30. Mohanty SS, Kumar A. Enhanced degradation of anthraquinone dyes by microbial monoculture and developed consortium through the production of specific enzymes. *Sci Rep*. 2021;**11**(1):7678. [PubMed ID: 33828207]. [PubMed Central ID: PMC8027401]. https://doi.org/10.1038/s41598-021-87227-6.
31. Ali RM, Hamad HA, Hussein MM, Malash GF. Potential of using green adsorbent of heavy metal removal from aqueous solutions: Adsorption kinetics, isotherm, thermodynamic, mechanism and economic analysis. *Ecological Engineering*. 2016;**91**:317-32. https://doi.org/10.1016/j.ecoleng.2016.03.015.
32. Oke IA, Olarinoye NO, Adewusi SRA. Adsorption kinetics for arsenic removal from aqueous solutions by untreated powdered eggshell. *Adsorption*. 2007;**14**(1):73-83. https://doi.org/10.1007/s10450-007-9047-z.
33. Wan Y, Liu X, Liu P, Zhao L, Zou W. Optimization adsorption of norfloxacin onto polydopamine microspheres from aqueous solution: Kinetic, equilibrium and adsorption mechanism studies. *Sci Total Environ*. 2018;**639**:428-37. [PubMed ID: 29793083]. https://doi.org/10.1016/j.scitotenv.2018.05.171.
34. Mohd Din AT, Hameed BH, Ahmad AL. Batch adsorption of phenol onto physiochemical-activated coconut shell. *J Hazard Mater*. 2009;**161**(2-3):1522-9. [PubMed ID: 18562090]. https://doi.org/10.1016/j.jhazmat.2008.05.009.
35. Kumar A, Jash A, Priyadarshinee R, Sengupta B, Dasguptamandal D, Halder G, et al. Removal of catechol from aqueous solutions by adsorption using low cost activated carbon prepared from Eichhornia crassipes. *Desalination and Water Treatment*. 2017;**73**:389-98. https://doi.org/10.5004/dwt.2017.20434.
36. Zhang Y, Zhu C, Liu F, Yuan Y, Wu H, Li A. Effects of ionic strength on removal of toxic pollutants from aqueous media with multifarious adsorbents: A review. *Sci Total Environ*. 2019;**646**:265-79. [PubMed ID: 30055489]. https://doi.org/10.1016/j.scitotenv.2018.07.279.
37. Lazo-Cannata JC, Nieto-Márquez A, Jacoby A, Paredes-Doig AL, Romero A, Sun-Kou MR, et al. Adsorption of phenol and nitrophenols by carbon nanospheres: Effect of pH and ionic strength. *Separation and Purification Technology*. 2011;**80**(2):217-24. https://doi.org/10.1016/j.seppur.2011.04.029.
38. Samadi A, Xie M, Li J, Shon H, Zheng C, Zhao S. Polyaniline-based adsorbents for aqueous pollutants removal: A review. *Chemical Engineering Journal*. 2021;**418**. https://doi.org/10.1016/j.cej.2021.129425.